

Received: 19 June 2021/ Accepted: 03 September 2021 / Published online: 09 September 2021

*freight car, qualities, CSM,  
polymer, vibration damping*

Assel KARASSAYEVA<sup>1\*</sup>, Yerzhan ADILKHANOV<sup>1</sup>,  
Sholpan SEKEROVA<sup>1</sup>, Saduakhas JAPAYEV<sup>1</sup>,  
Algazy ZHAUYT<sup>1</sup>, Seitbek ZHUNISBEK<sup>1</sup>, Kazhybek TERGEMES<sup>1</sup>

## **ANALYSIS OF DYNAMIC PROPERTIES AND MOVEMENT SAFETY OF BOGIES WITH DIAGONAL LINKS AND RUBBER-METAL VIBRATION ABSORBERS BETWEEN THE RUBBING ELEMENTS OF FREIGHT CARS**

This article aims to study experimentally the dynamic properties and traffic safety actions for gondola cars with bogies with diagonal links, operated on the territory of the Republic of Kazakhstan. The main results obtained during tests of gondola cars on bogie with diagonal links when they move along straight and curved sections as well as on switches are presented. The estimation of: dynamics coefficients, stability margin coefficients against derailment, lateral forces transmitted from the wheel to the rail, ratio of frame forces to a static load from the wheelset on the rails, and accelerations are made. The paper analyses the simulation of a polymer layer of rubber vibration absorber, to be installed between the rubbing surfaces, such as the link side of frame axle unit, and host unit is open-bearing, with lateral support of the three-piece freight car bogies, operating on the territory of the Commonwealth of Independent States. The model developed in this article consists of a rheological model of a Maxwell cell, a Fancher spring and an element which has the function of non-linearity. The simulation model can be used to study the characteristics of vibration dampers, gaskets and other power elements that have polymer properties and are installed at other types of transport and not only.

### **1. INTRODUCTION**

On the railways of the Republic of Kazakhstan, the Russian Federation and other countries of the Commonwealth of Independent States, freight wagons are mainly used on bogies 18-100 (CNII-X3), designed according to the “standards of the way content” of 1950, tested in 1952 and produced serially from 1956 till the present. For freight wagons on CNII-X3 bogies, the characteristic position when moving in a circular curve is the contact of the first wheelset with the curved track outer rail [1]. In this case, not only the natural rotation of the bogies under the car body is observed, but also an undesirable phenomenon called “running” (or “overtaking”) of the bogies side frame in the curve when the bogie adopts the parallelogram configuration in the plan [2]. If the bogie is significantly

---

<sup>1</sup> Electronics and Robotics, Almaty University of Power Engineering and Telecommunications, Kazakhstan

\* Email: ali84jauit@mail.ru

<https://doi.org/10.36897/jme/141926>

skewed, contact may also occur with the flange of wheel of the second wheelset of the bogie. This position of the bogie in the rail track was called the jammed wedge [3].

The geometry of the bogies of the freight wagon when it moves in a circular curve leads to the fact that the reaction to the inertia force acting on the crew is concentrated in the contact area of the outer wheel of the first wheelset with the rail. A large value of the transverse force acting between the wheel and the rail can lead to the lifting of the wheel and descent of wagon from the rails [4]. Increased safety of movement in the curve is possible by redistributing the inertia force of the crew between all the outer wheels [5]. This is possible if the crew's wheelsets occupy a radial position in the circular curve. At angles of attack of a wheelset on a rail no more than 5 mrad, the entry of a bogie into a curve is considered to be close to a radial one [6]. Experience shows that the main way to reduce the shift of side frames relative to each other and to ensure the self-centering wheelsets in curved sections of road is the equipment of the carriages with additional links. Theoretical foundations for the creation of bogies with self-centering wheelsets were laid by A. Wickens and H. Scheffel. This includes the bogie model 18-9996 (ZK-1), which since 2008 is in operation on the railways of the Republic of Kazakhstan. The fundamental difference between the 18-9996 (ZK-1) model of bogie and the main models of three-piece bogies consists in the availability of diagonal links between the side frames, which increase the longitudinal rigidity of bogie in the plan view and accordingly reduce the longitudinal overshoot of the side frames relative to each other and provide self-centering in curved sections [7]. As a result, the intensity of the bogie wobble is reduced, and the smoothness of the bogie running is improved. The largest number of studies devoted to such designs was carried out by Professor H. Scheffel. The 18-9996 (ZK-1) bogie models was first mentioned in [8]. In the results of tests of cars with bogies with diagonal links are given however, only the dependences of the vertical and horizontal coefficients on the speed of movement are given, and this does not allow making unambiguous conclusions, assessing the degree of influence on the railway track and the safety of movement of cars on bogies of 18-9996 (ZK-1) model [9]. In this regard, the authors of this article analysed the results of experimental studies conducted on straight, and curved sections and on switches with cross piece of grades 1/9 and 1/11. According to the results of data processing at a given speed, separate data arrays were formed for each measuring circuit [10]. These arrays were used to find the estimated parameters. All measurements were classified by speed. In each run, one maximum amplitude value of the dynamic process was selected [11]. Side forces, the ratio of frame forces static load from the wheelset rails, the stability criterion of the rail grate from shear, the coefficients of stability margin against the derailment of the wheel and the smoothness of ride were taken as evaluation parameters [12].

## 2. MATERIALS AND METHODS

Freight cars operating on the territory of the Commonwealth of Independent States are equipped with so-called three-piece bogies. They are called three-piece because the bogie consists of two side frames and a bolster [13]. The main representative of three-piece bogies – the bogie model 18-100 or TsNII-X3 was designed in the fifties of the last century

(see Fig. 1). Since the end of the 90s, due to the urgent need, research and design organizations have made designs of various bogies of freight cars with improved dynamic properties and increased turnaround time [14]. One of them is a bogie model 18-9996 (ZK-1), which rolls under gondola cars produced in the Republic of Kazakhstan (see Fig. 2b).



Fig. 1. Bogie model 18-100 (TsNII-X3)

Since the beginning of the XX century, due to urgent need, research and design organizations have developed projects for various bogies of freight cars with improved dynamic qualities and increased inter-repair mileage. Variants of bogies with reinforced load-bearing elements, elastic-roller support devices (sliders), central spring suspension with a modified vibration damping system, a modified link side frame and the axle box, etc. are proposed. Currently, pliable rubber-metal elements installed between axle box and side frame are widely used. Such elements are executed both in the form of simple polyurethane overlays and in the form of multilayer rubber-metal gaskets. In the process of operation they implement flexibility in three linear and three angular directions. Some of these bogies are shown in Fig. 2.

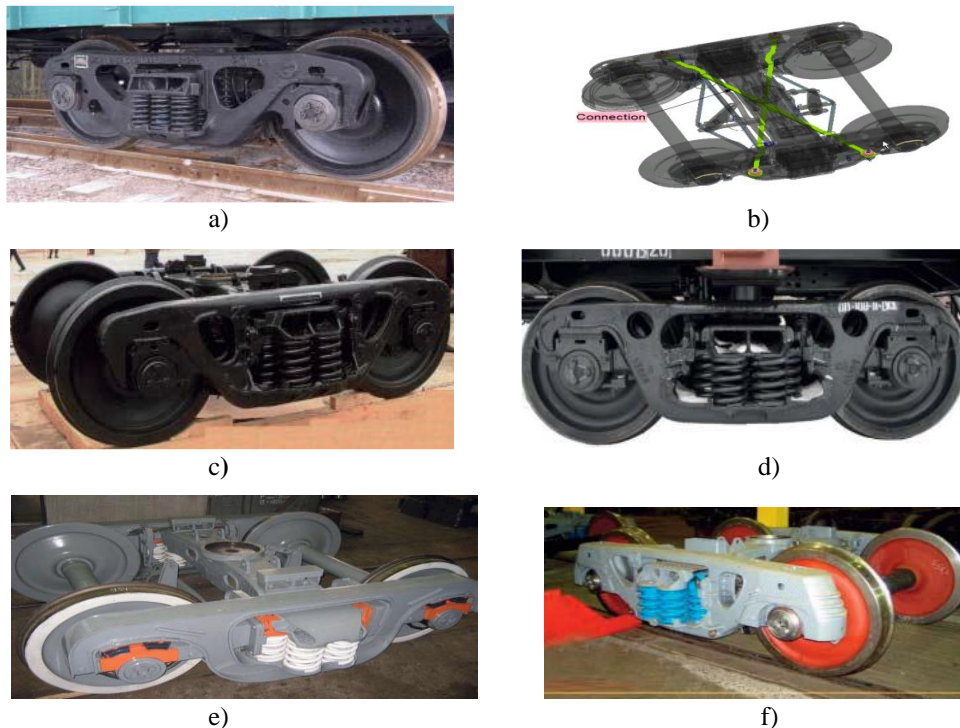


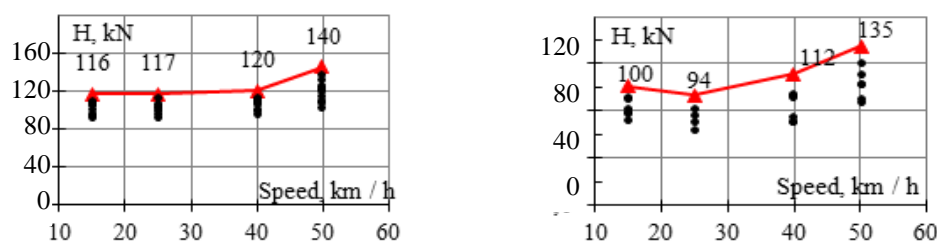
Fig. 2. Bogie models: a) 18-9810 (Russia), b) 18-9996 (China), c) 18-194 (Russia), d) 18-9800 (Russia), e) 18-9750 (Russia), f) 18-4129 (Ukraine)

Paper [15] is devoted to studies of influence of elastic and dissipative parameters on dynamics and wear indicators. Basically, linear Voigt models are used for modelling elastic elements, consisting of parallel linked elements of elasticity and viscosity. However, bogie models shown above are expensive and only a few of them have been put into mass production. Despite the theoretically and experimentally proven possibility of creating bogies that are friendly to road, the bogies that largely repeat the technical solutions of previous years adopted abroad are put into production in countries of independent states (CIS). Bogies offered by various manufacturers solve problem of improving the durability, driving performance and safety of cars in their own way. They have a different arrangement of the axle box or adapter, a wear-resistant element of the axle box assembly, a side frame, suspension springs, friction wedges, a spring beam, and side sliders and are unified only in wheelsets, cassette bearings and brake lever transmission. New solutions are mainly associated with the introduction of wear-resistant elements in pairs of friction and shock absorbers of non-gapped sliders. The appearance of a large number of different types of bogies, which are not fundamentally different in their capabilities, will cause additional costs in operation.

Table 1. Defined characteristics of bogies

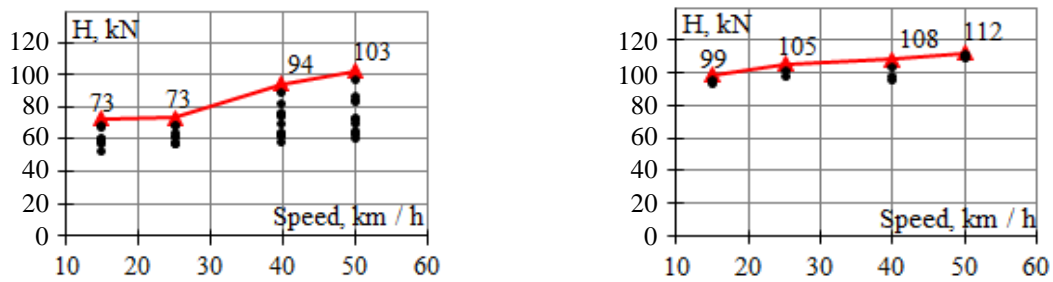
Name of defined characteristics	Standard value
Permissible lateral forces transmitted from wheel to rail, ( $H$ ): - in straight lines, curves and turnouts on wooden sleepers; - in switches on reinforced concrete sleepers.	no more than 100 kN no more than 120 kN
Shift resistance of rail-sleeper grate, ( $\alpha$ )	no more than 1.4
Permissible ratio of frame force to vertical static load of wheelset on rails, ( $Y/F_A$ )	no more than 0.3
Coefficient of stability margin against derailment of wheels with rails	not less 1.4
Smoothness degree	4

Lateral forces were evaluated only in the loaded mode on switches and a curved sections of track [16]. To register the lateral forces from the wheel to the rails, a bridge scheme using the Schlumpf method is applied. A special load device with force-measuring sensors was used for calibration of strain-measuring schemes for measuring lateral and vertical forces [17]. In the test on switches, the forces transmitted from the wheel to the rails in the horizontal direction were measured in the forward reach of the frame rails and in the diverging curve [18]. Thus, Figures 3–5 show the dependence of the lateral forces transmitted from the wheel to the rails on the speed of movement.



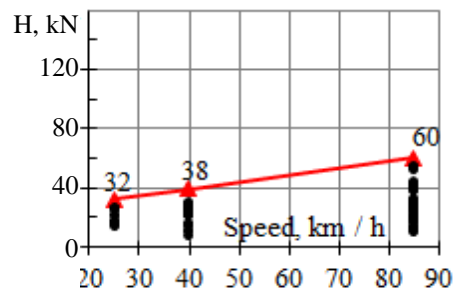
- – observed values; —▲— maximum probable value of a quantity;  $H = H_A + 3S$ ;  $H_A$  – the average value of the lateral force for the relevant speed;  $S$  – lateral force standard deviation

Fig. 3. Lateral forces from wheelset on rails for cross piece 1/9 diverging curve (left) and frame rail (right)



- – observed values;    ▲ – maximum probable value of a quantity;  $H = H_A + 3S$ ;  $H_A$  – the average value of the lateral force for the relevant speed;  $S$  – lateral force standard deviation

Fig. 4. Lateral forces from wheelset on rails for cross piece 1/11 diverging curve (left) and frame rail (right)



- – observed values;    ▲ – maximum probable value of quantity;  $H = H_A + 3S$ ;  $H_A$  – the average value of the lateral force for the relevant speed;  $S$  – lateral force standard deviation

Fig. 5. Lateral forces from wheelset on rails for curved section

Analysis of the data shown in Figures 3–5 showed that the greatest lateral forces are usually caused by the action of the guide wheelsets in the bogie [19]. In addition, the observation revealed that the level of impact path of a loaded gondola car was 3–4 times higher than the level of impact on the path of an empty gondola car [20]. In the diverging curve of the 1/9 cross piece switch, the excess of permissible threshold of lateral forces was registered when moving a loaded gondola car at a speed of 50 km/h (Fig. 3, left). When moving a loaded gondola at a speed of 40 km/h, the lateral forces reached the maximum permissible thresholds. In this regard, it is recommended to limit the permissible speed of a loaded gondola car with 1/9 cross piece switches in the diverging direction to a speed of 35 km/h. When driving on switches with a 1/9 and 1/11 cross piece in the forward direction [21], the impact indicators on the path were not exceeded. Further, the calculation method allows determining the stability values of rail-bar grid against laterally shifting ballast, which is estimated by the ratio of the maximum horizontal load to the average vertical load of the rail on the bar and is calculated by the formula according to:

$$\alpha = \frac{H_s^{\max}}{F_s} \quad (1)$$

Table 2. Stability calculating results for rail and bar grate against lateral shear by ballast in turnout switch with 1/9 cross piece

Speed, km/h	Wheelset numbers							
	1	2	3	4	1	2	3	4
	Empty				Laden			
15	1.33	0.51	1.39	0.53	1.31	0.86	0.84	0.80
25	1.15	0.64	1.35	0.65	1.25	0.80	0.68	0.84
40	1.26	0.63	1.38	0.63	1.32	0.93	1.03	0.66
50	<u>1.82</u>	0.58	<u>1.95</u>	0.75	1.32	0.95	1.11	0.83

Table 3. Stability calculating results for rail and bars from lateral shear by ballast in turnout switch with 1/11 cross piece

Speed. km/h	Wheelset numbers							
	1	2	3	4	1	2	3	4
	Empty				Laden			
15	1.31	0.66	1.39	0.49	1.05	0.40	0.85	0.41
25	1.19	0.71	1.31	0.64	1.00	0.40	0.84	0.47
40	1.38	0.63	1.38	1.03	1.26	0.54	1.03	0.58
50	<u>1.83</u>	0.66	<u>1.58</u>	0.86	1.14	0.50	0.98	0.47

Calculations showed that when moving along turnouts with 1/9 and 1/11 cross piece in the diverging direction at a speed of 50 km/h, an excess of the permissible value criterion for the stability of the rail and bar grate against lateral shear ballast had been found [22]. When driving at a speed of 40 km/h and below, the excess was not detected. When driving on a curve and straight sections of the path, no excess was found [23]. The values of frame forces took into account the quasi-static component. The dependencies of ratios of frame forces to the static load from the wheelset on the rails on the speed of movement are shown in Figs. 6 and 8.

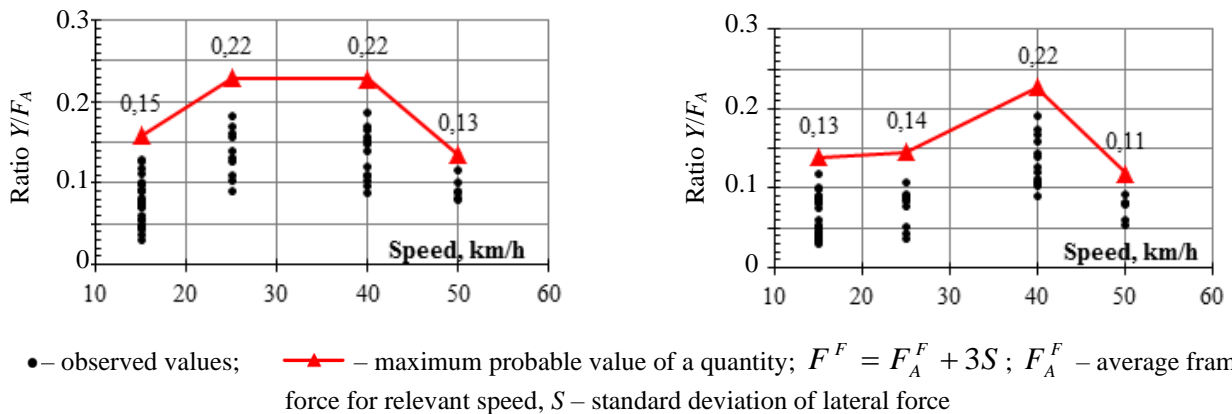


Fig. 6. Ratio of frame forces to static load from wheelset on rails for cross piece 1/9 of gondola car in unladen (left) and loaded (right) states

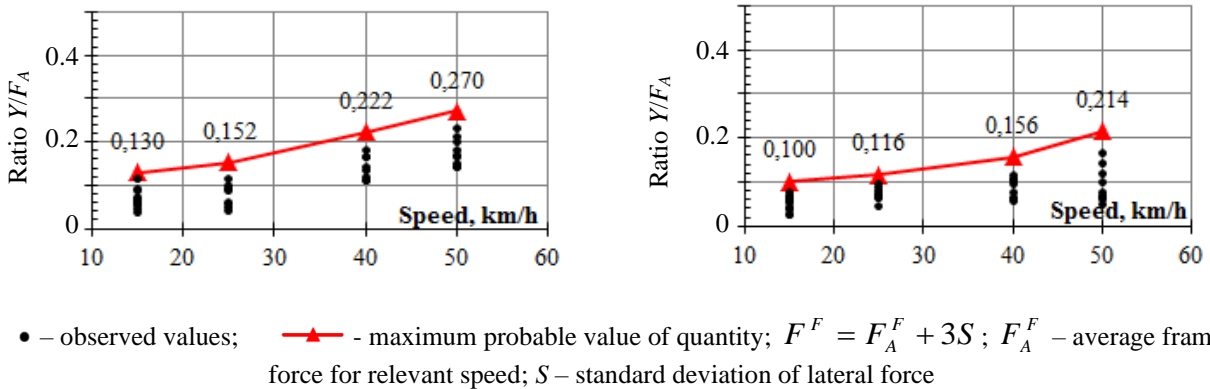


Fig. 7. Ratio of frame forces to static load from wheelset on rails for cross piece 1/11 of gondola car in unladen (left) and loaded (right) states

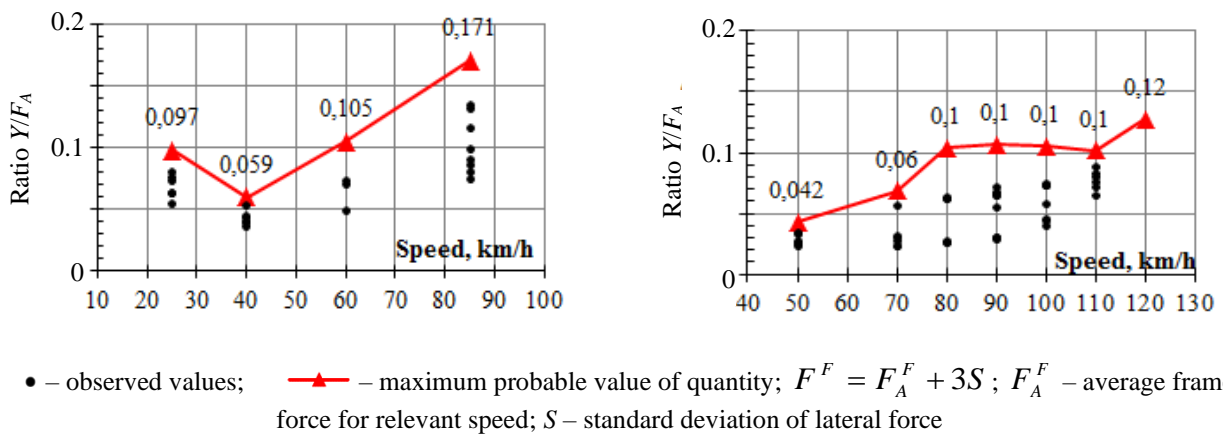


Fig. 8. Ratio of frame forces to static load from wheelset on rails of loaded gondola car for curve (left) and straight line (right)

Figures 6–8 show ratios of frame forces to the static load from the wheelset on the rails when moving gondola cars with switches are within acceptable values [24]. There is also a noticeably greater dynamics in the empty car [25]. Then, using instantaneous values of frame forces and the coefficient of vertical dynamics of the first stage of spring suspension, the values of the coefficient of stability margin against wheel derailment were calculated using the formula:

$$CSM = \frac{tg\beta - \mu}{\mu \cdot tg\beta + 1} \cdot \frac{F_V}{F_H} \geq [1,4] \tag{2}$$

where:  $CSM$  – is the coefficient of stability margin;  $\mu$  – is the coefficient of friction between the oncoming wheel ridge and the rail;  $\beta$  – is the angle of inclination of the forming wheel ridge to the horizontal plane  $\beta = 60^\circ$ ;  $F_V$  – is the vertical load of the wheel on the rail;  $F_H$  – is the horizontal load from wheel to rail. The coefficient of stability margin was estimated by the minimum calculated value only in the empty mode (Figures 9–10).

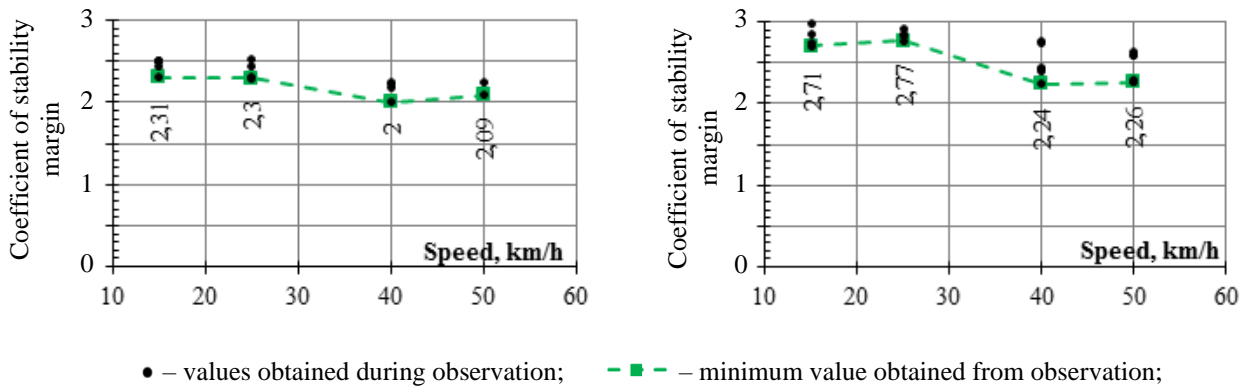


Fig. 9. Coefficient of stability margin derailing wheel from rail when empty gondola car passes turnouts of 1/9 (left) and 1/11 (right)

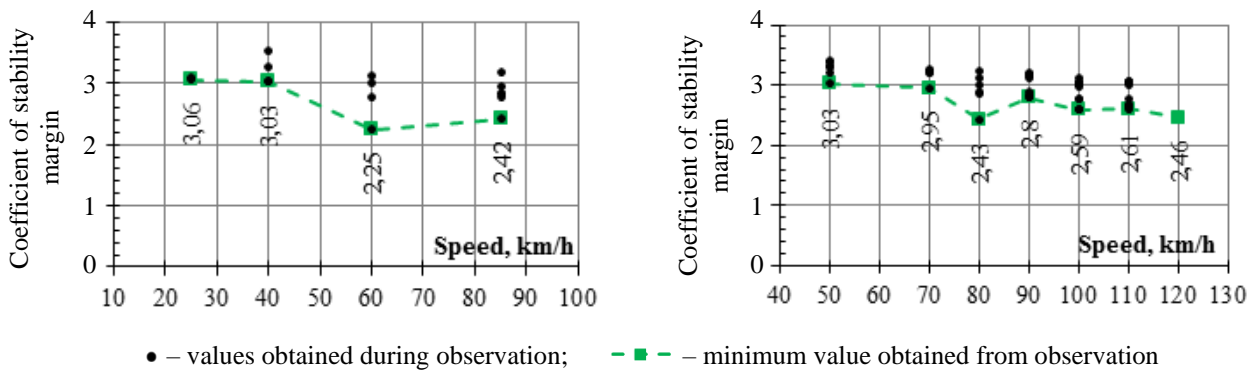


Fig. 10. Coefficient of stability margin derailment wheel from rail when empty gondola car passes curve (left) and straight (right) lines

The dependencies shown in Figures 9–10 demonstrate that the coefficient of stability margin against derailment of the wheel when gondola passes switches on the diverging and through sections of the track are within acceptable limits, i.e. At the next stage [26], based on the accelerometers installed on the body of the gondola cars, the smoothness indicators for a straight section of bogie were calculated. The results are shown in Figures 11–12.

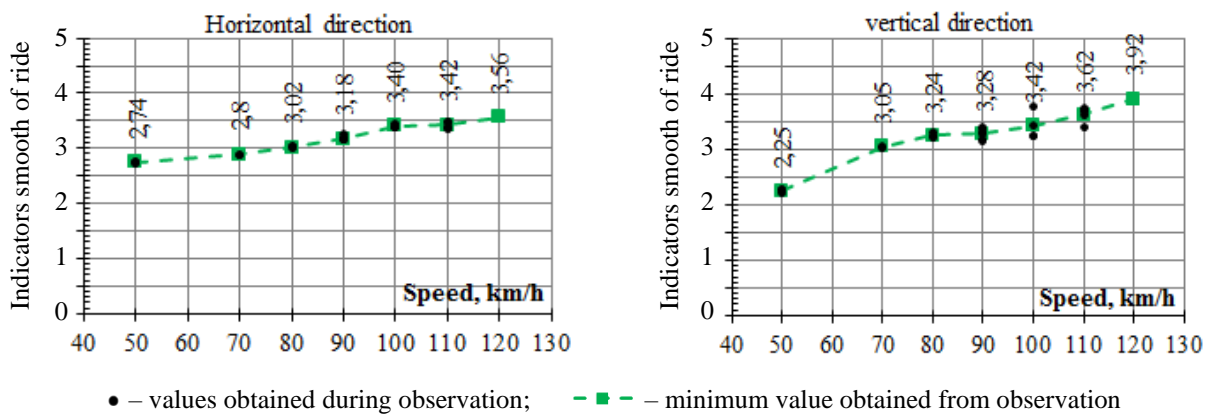


Fig. 11. Indicators smoothness of ride empty gondola on straight section

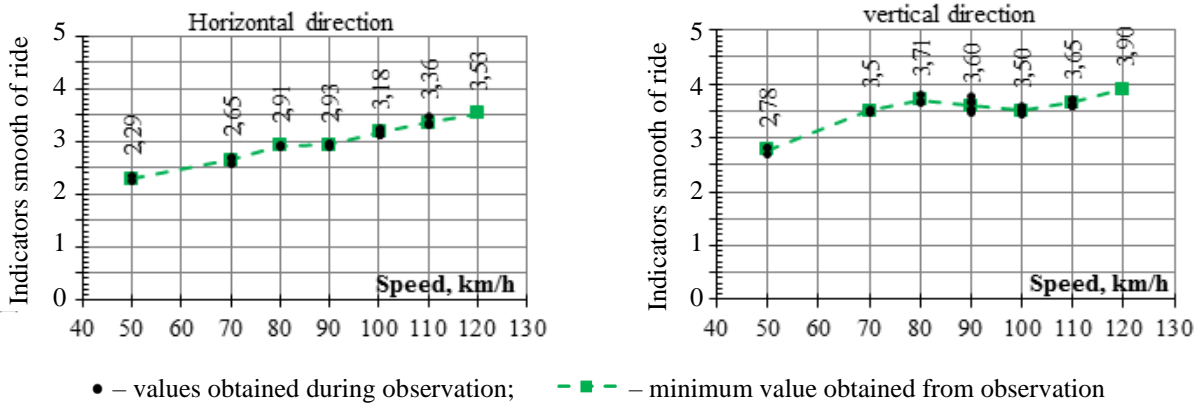


Fig. 12. Parameters smoothness of ride laden gondola car on straight section

The results shown in Figures 11–12 demonstrate that the smoothness indicators of open-top wagons on straight sections of the bogie meet the requirements when moving at speeds up to the design speed.



Fig. 13. General view of axle-box adapter with a wear-resistant vibration absorber

A general view of axle box adapter, with a wear-resistant vibration absorber installed on it, is shown in Fig. 13. Rubber-metal elements installed between the axle-box and the side frame - such elements are made both in the form of simple polyurethane linings and in the form of multilayer rubber-metal gaskets [27]. During operation, they ensure mutual compliance in three linear and three angular directions. However, the proposed model is simple in design and can be installed between the axle-box and the side frame without making changes to the bogie design [28]. To reduce wear in friction units and consequently, the overhaul mileage of the model 18–100 bogie shall be increased. So it is proposed to install vibration absorbers made in the form of three-layer gaskets, consisting of two steel and one polymer or rubber layers between the axle-box and the side frame (Fig. 14).

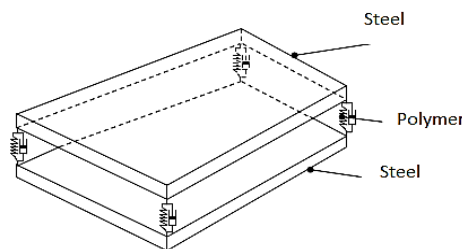


Fig. 14. Three-layer rubber-metal vibration absorber

In this article, a simulation model of a polymer layer of a rubber-metal vibration absorber is considered. The polymer layer was implemented using the Maxwell rheological model, the Fancher spring model and the non-linearity element (Fig. 15).

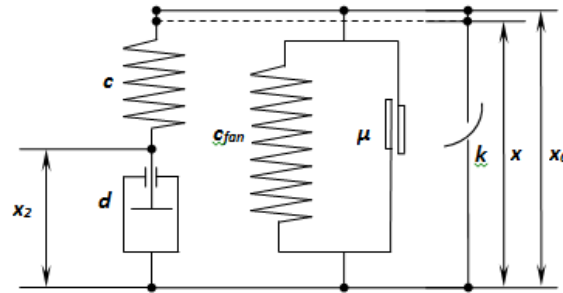


Fig. 15. Diagram of polymer model

The Maxwell model is a serial link of a linear spring and a damper, which is used mainly for modelling vibration dampers and in parallel link with other types of elements – for modelling rubber-metal elements, elastomers and so on [29]. The mathematical model is constructed from the condition of equality of elastic and elastic-dissipative forces and due to inertia-free force element and includes the differential equation:

$$d \cdot \dot{x}_2 = C \cdot x_1 \tag{3}$$

where:  $C$  – is the spring constant;  $d$  – is the dissipation of a viscous element.  $x_2 = x - x_1$ .

The mathematical model of the Plywood spring, which is a modification of the rheological model of a parallelly installed spring and dry friction damper, is constructed as follows:

$$F_{fan.i} = F_{bnv.i} + (F_{fan.i-1} - F_{bnv.i-1}) e^{-|\Delta_{xi} - \Delta_{xi-1}| / \beta} \tag{4}$$

$$F_{env.i} = -C_{fan} \cdot \Delta_{xi} - F_{fr} \cdot \text{sign}(\Delta_{xi} - \Delta_{xi-1}) \tag{5}$$

$$F_{fr} = \mu \cdot C_{fan} \cdot \Delta_{xi} \tag{6}$$

$$\Delta_{xi} = x_i - x_{0i}$$

where:  $F_{fan,i}$ ,  $F_{fan,i-1}$  – are the power at the current and previous integration step, respectively;  $\Delta_{xi}$ ,  $\Delta_{xi-1}$  – is the difference in deformations at the current and previous integration steps respectively;  $F_{bnv,i}$ ,  $F_{bnv,i-1}$  – is the maximum force value when increasing  $x$  (minimum value when decreasing  $x$ ) on  $x_i$ ;  $\mu$  – is the coefficient of friction;  $C_{fan}$  – is the spring stiffness;  $F_{fr}$  – is the friction force;  $\beta$  – is the exponential parameter of suspension (delay).

To implement non-linearity (changes in stiffness due to deformation), an element described by the dependency is set in parallel with the two elements described above:

$$F_n = \pm k \cdot (x - x_0)^3 \tag{7}$$

where:  $k$  – is the coefficient of non-linearity; “+” when soft characteristic occurs; “-“ when it is hard,  $M \times N/m^3$ .

### 3. RESULTS AND DISCUSSION

In order to check the adequacy of the developed computer model [19], the hysteresis obtained during testing of a real polymer material was compared (see Fig. 16) with the hysteresis obtained by modelling (static loading at the following values of indicators:  $\mu = 0.8$ ;  $C = C_{fan} = 9 \cdot M \times N/m$ ;  $\beta = 0.000002$ ;  $k = -6 \cdot 10^{12} \text{ N/m}^3$ ;  $f = 0.01 \text{ Hz}$ ;  $d = 4500 \text{ N} \times \text{s/m}$ ), see Fig. 5.

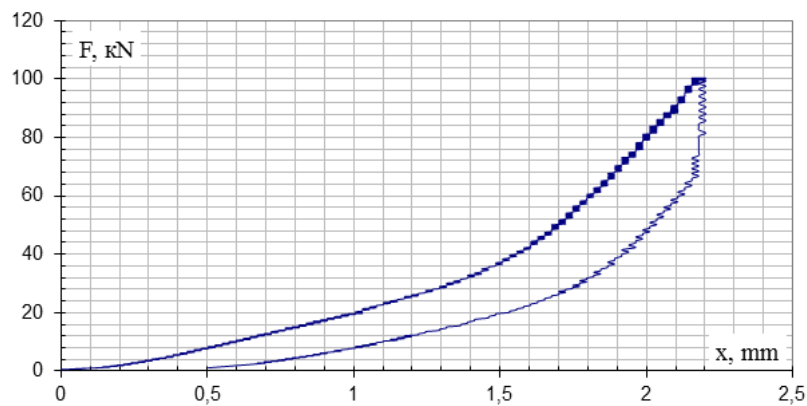


Fig. 16. Stress-strain diagram of polymer (experiment)

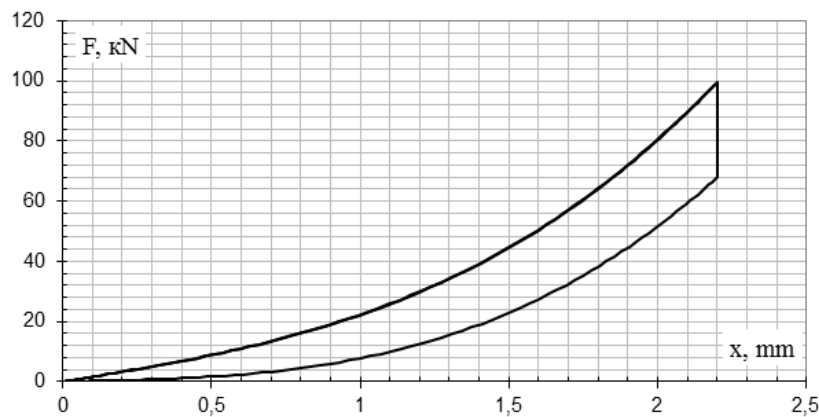


Fig. 17. Polymer deformation diagram (modelling)

As it can be seen from Figs. 16 and 17 the developed model allows us describing the polymer material fairly accurately [20]. In addition, at this stage, it does not matter what value the dissipation parameter  $d$  will have, since static loading has been performed at a low frequency. Next, the influence of each system parameters will be studied [21]. At the first stage, the influence of the nonlinearity parameter and delay will be investigated by modelling the system with a perturbation of the type:

$$Z = -\frac{A}{2}(1 - \cos(\omega t)) \quad (8)$$

where  $A$  – is the oscillation amplitude;  $\omega$  – is the oscillation frequency.

Thus, Fig. 18 shows the simulation results for different values of the nonlinearity coefficient  $k$ , for  $\mu = 0.25$ ;  $C_{jam} = 9 \cdot M \times N/m$ ;  $\beta = 0.000002$ ;  $f = 0.01$  Hz;  $A = 10$  mm.

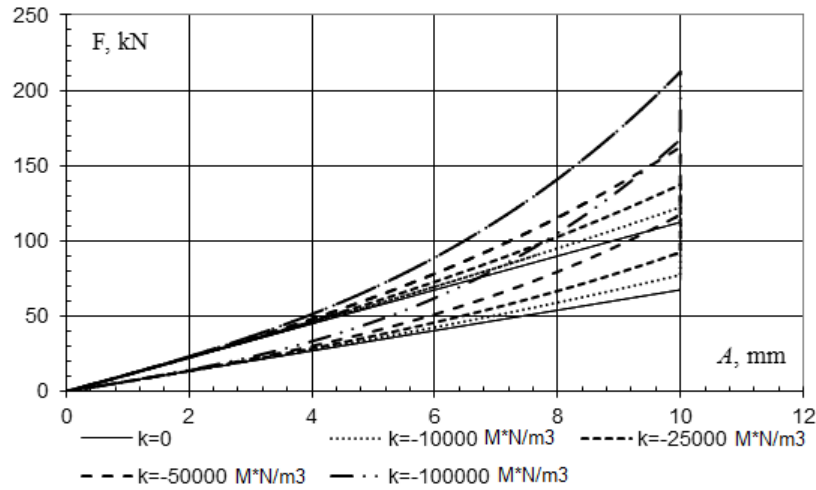


Fig. 18. Dependences of force on element deformation

The hysteresis shows that an increase in the non-linearity coefficient leads to an increase in stiffness depending on the deflection, which is typical for polymer materials [22]. The value of the friction force remains unchanged. Next the effect of the delay parameter  $\beta$  will be evaluated. Fig. 19 shows the simulation results.

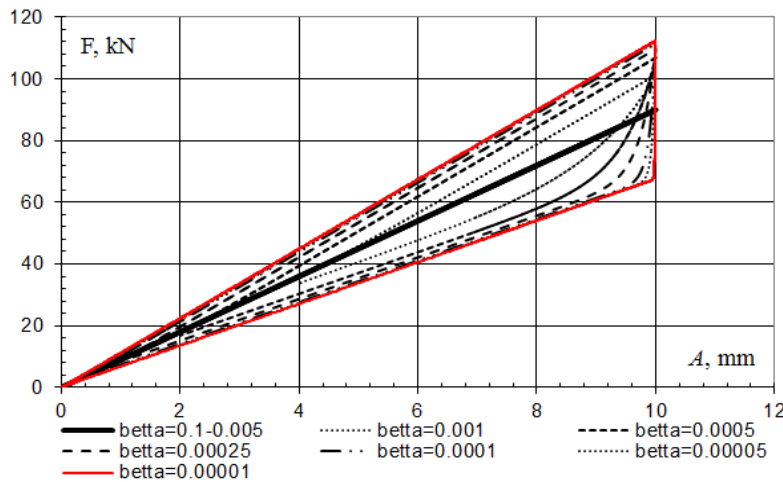


Fig. 19. Dependences of force on element deformation

The influence of the delay parameter mainly affects the amount of friction forces and the area of hysteresis. If  $\beta \rightarrow 0$  is desired, the element implements the characteristic of the friction force depending on the load [24]. It is known that the dissipative properties of rubber and polymer materials depend on the frequency. Therefore, the next step was to

evaluate the influence parameters of the Maxwell element. To do this, the change of the variable  $z$  is considered according to the harmonic law:

$$Z = x_0 + A \cdot \sin(2\pi ft)$$

$$\dot{Z} = 2\pi f A \cdot \sin(2\pi ft)$$

where:  $x_0$ ,  $A$ ,  $f$  – are the center of vibrations; their amplitude and frequency (Hz). The response of a force element to a perturbation is the periodic force:

$$F(t) = F(z(t), \dot{z}(t))$$

If the dependence is decomposed into a Fourier series, keeping only the zero and the first terms of the series, it can be gotten:

$$F(t) \approx F_0 - F_k(f) \sin(2\pi ft) - F_c(f) \cos(2\pi ft) = F_0 - F_1(f) \sin(2\pi ft - \delta(f))$$

Based on this representation, the main characteristics of the power element in the frequency domain are introduced as:

- dynamic stiffness  $K(f) = F_k(f) / A$ ,
- equivalent damping coefficient  $C(f) = F_c(f) / 2\pi f A$ ,
- phase or angle of dissipation  $\delta(f)$ .

Since the forces in the elements are the same when connected sequentially. two obvious relations are obtained from expression in Eq. (8):

$$x_1 = F / C \quad \dot{x}_2 = F / d$$

If the relations are differentiated. a relationship is gotten between the strain and the force:

$$\dot{x} = \dot{F} / C + F / d$$

At a constant load, the force  $F$  in the element is constant therefore, the deformation rate is also constant, and the deformation is not limited by anything. The effect of frequency and dissipation is considered at a fixed value  $C = 9 \cdot \text{M} \times \text{N} / \text{m}$ . Thus Fig. 20 shows the dependence of the force on the strain at different values of the frequency  $f$  at a fixed value  $d = 1000 \text{ N} \times \text{s} / \text{m}$ .

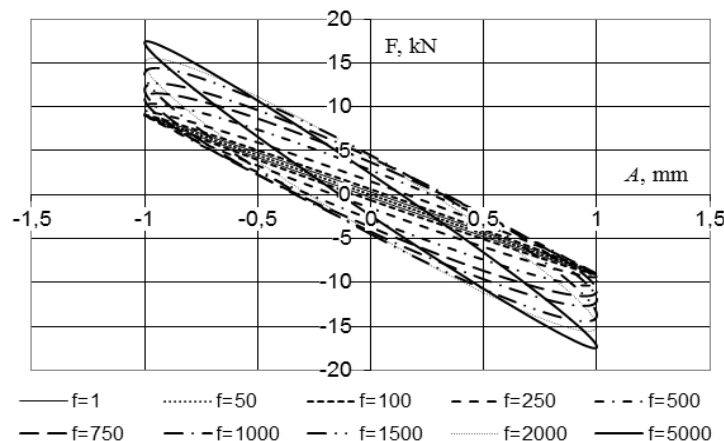


Fig. 20. Dependences of force on deformation of element at different frequencies ( $f$  Hz)

From the dependencies shown in Fig. 9., it can be seen that with increasing frequency, there is an increase in dynamic stiffness (the angle of inclination of the dependencies in the figure) and the absorbed energy [25]. However, an excessive increase in frequency results in a reverse decrease in damping [26]. Thus, Figs. 21 and 22 show the dependences of attenuating vibrations of a body with a mass of 10 t (the approximate mass per axle-box unit in loaded mode) from time to time for different dissipation values [27].

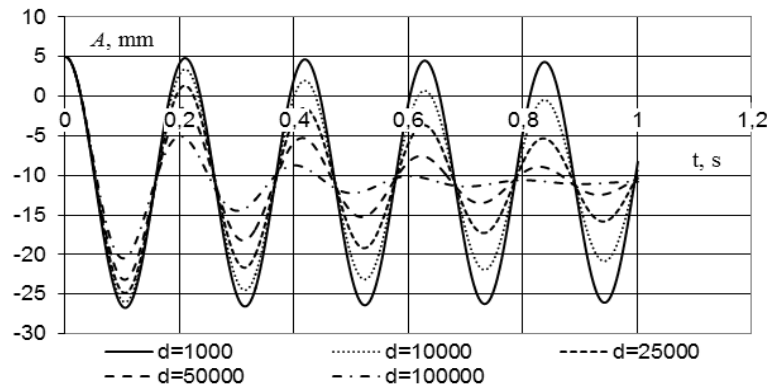


Fig. 21. Damped oscillations ( $d$  kN×s/m)

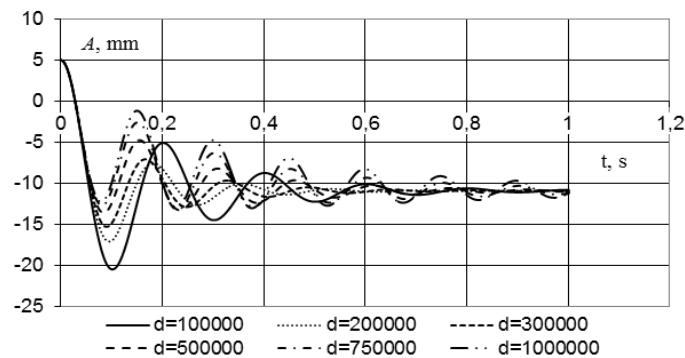


Fig. 22. Damped oscillations ( $d$  kN×s/m)

Results in Figs. 21 and 22 clearly show that with the stiffness of a sequential spring with  $C = 9\text{M}\times\text{N/m}$ , there is no complete damping of vibrations, i.e. there are no aperiodic vibrations. In this regard, the influence of the dissipation parameter in the frequency domain is further evaluated. Figs. 23 and 24 show the simulation results depending on the frequency of vibrations.

It follows from Figs. 23 and 24 that an increase in the dissipation factor leads to a decrease in the dependence of parameters  $c$  and  $d$  on frequency. It should be noted that the value of  $\tau = d/C$  in rheology, it is called the relaxation time [28]. Therefore, the shorter the relaxation time is the more sensitive the element is to the frequency of vibrations [29]. Thus, by varying the ratio of  $C$  and  $d$ , it is possible to determine the frequency limit at which maximum damping should be achieved.

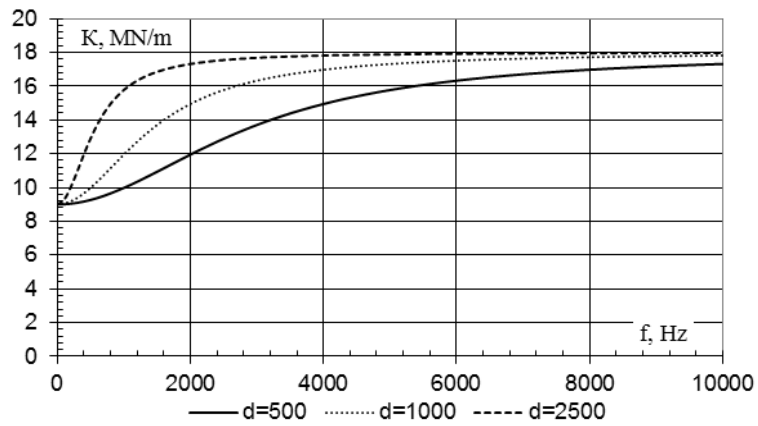


Fig. 23. Dependence of dynamic stiffness on frequency ( $d$  kN\*s/m)

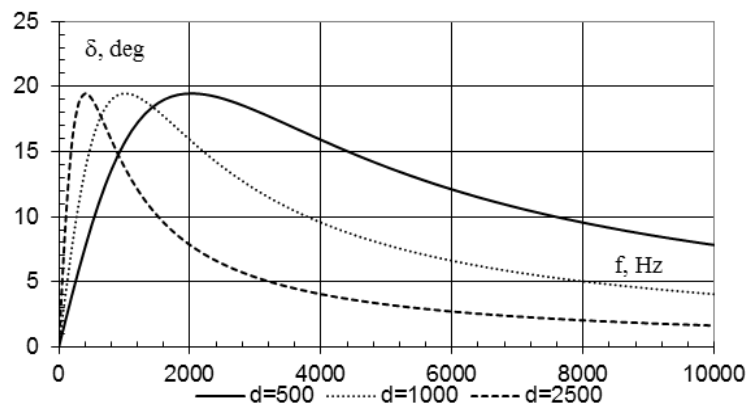


Fig. 24. Dependence of angle of dissipation on frequency ( $d$  kN\*s/m)

At the final stage, free vibrations of the cargo with weights of 50 and 10000 kg were simulated, respectively. Results obtained when  $d = 4.5$  kN\*s/m and 100 kN\*s/m and the non-linearity coefficient  $k = -6 \cdot 10^{12}$  N/m<sup>3</sup> without friction and with friction, shown in Figs. 25 and 28.

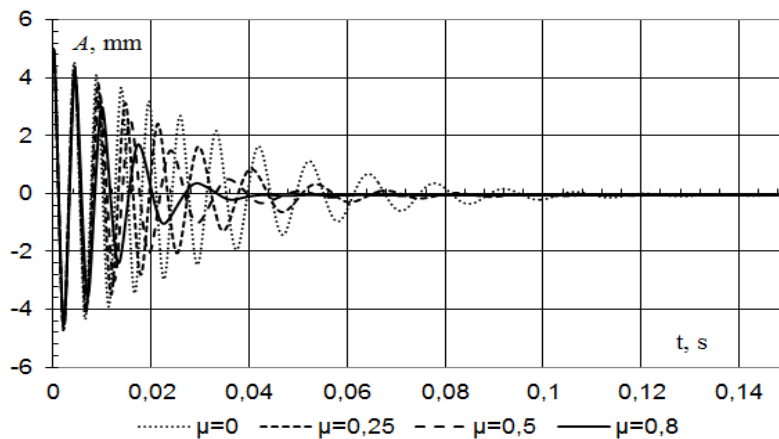


Fig. 25. Damped oscillations at  $m = 50$  kg ( $C = 9 \cdot M \cdot N/m$ ;  $d = 4.5$  kN\*s/m)

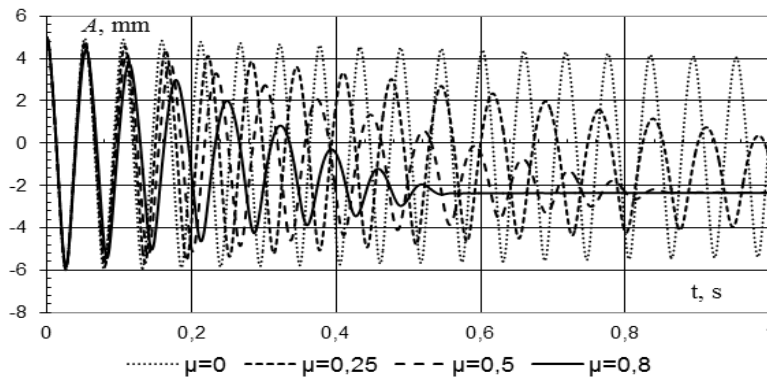


Fig. 26. Damped oscillations at  $m = 10 \text{ t}$  ( $C=9 \cdot M \times N/m$ ;  $d = 4.5 \text{ kN} \times \text{s}/m$ )

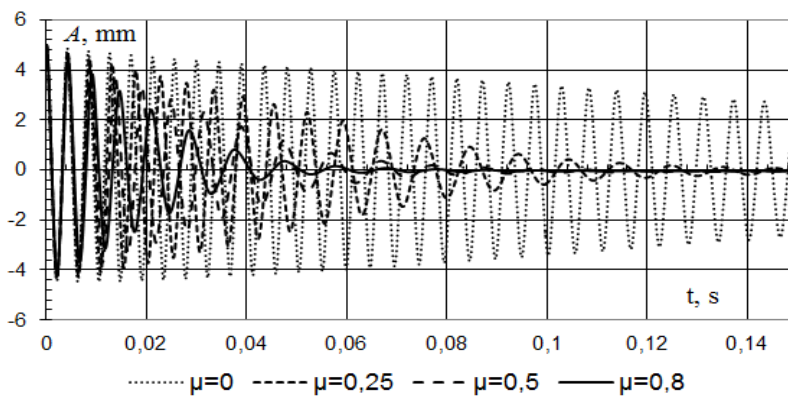


Fig. 27. Damped oscillations at  $m = 50 \text{ kg}$  ( $C = 9 \cdot M \times N/m$ ;  $d = 100 \text{ kN} \times \text{s}/m$ )

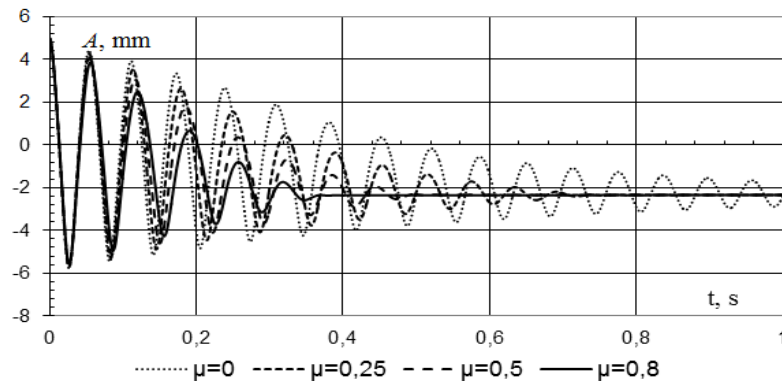


Fig. 28. Damped oscillations at  $m = 10 \text{ t}$  ( $C = 9 \cdot M \times N/m$ ;  $d = 100 \text{ kN} \times \text{s}/m$ )

The next phase was produced by computer simulation of car movement with two axle unit options: option 1 – model of the standard bogie; option 2 – model of the bogie with an upgraded adapter with anti-vibration absorber and comparing the results. The research was bogie out with help of developed refined computer models of different types of freight cars [1], created in the software environment of the “Universal Mechanism” complex [29], which includes a developed module for analysing dynamics of railway bogies (see Fig. 29).

The obtained results of numerical modelling were processed and averaged values in percent for curves and straight sections were obtained, taking into account the load of car. As criteria for assessing the impact of selected options of axle-boxes, indicators of dynamic qualities (dynamics coefficients level of lateral and frame forces), traffic safety (the margin of stability of wheels against derailment) and wear in the friction units of bogie (wear parameters of friction pairs).

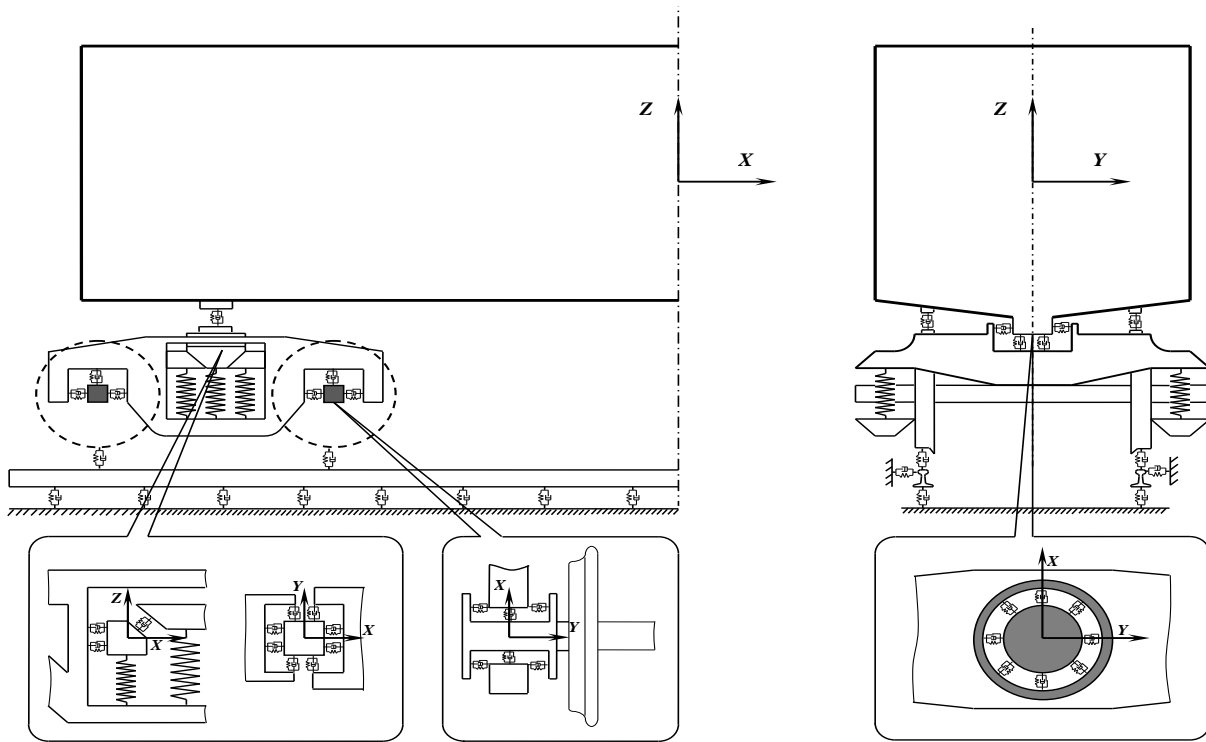


Fig. 29. Structure of the half-car physical model

In Figs. 30 and 31 shows results in percent compared to the base model variant of axle unit (value “-” i.e. decrease means improvement compared to the baseline).

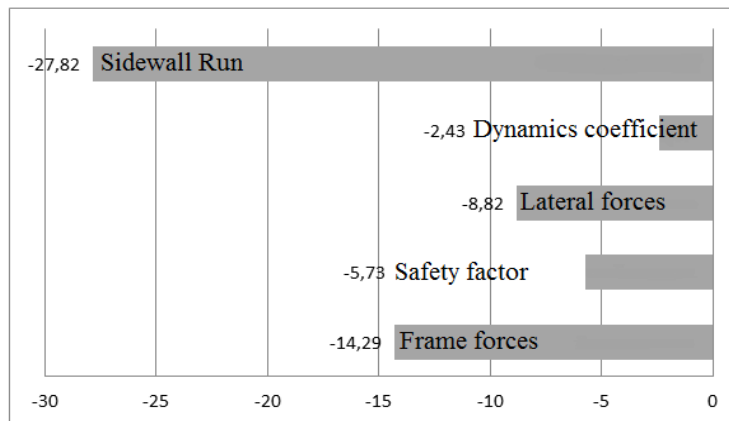


Fig. 30. Average values of dynamic parameters of driving qualities in comparison with a typical bogies

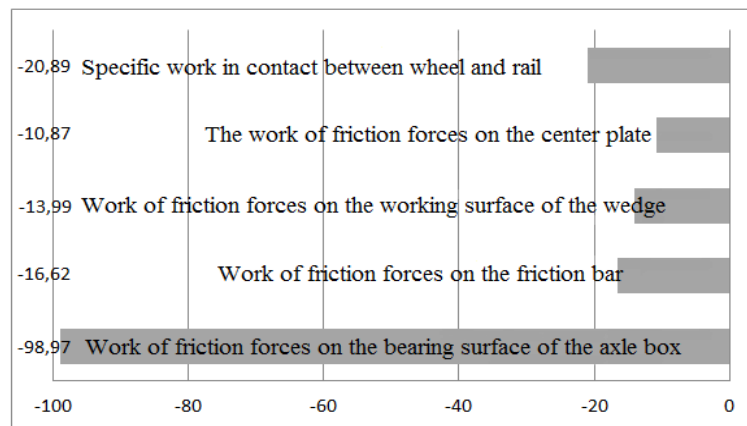


Fig. 31. Average values of wear indicators compared to a typical bogies

Analysis of the average values of dynamics and safety indicators showed that a positive effect is achieved when using a wear-resistant vibration absorber. In terms of wear indicators, the maximum effect is achieved by reducing wear of the support surface axle-box assembly by almost 2 times (by 99%) and the rolling profile of wheel and rail head by 21%.

## CONCLUSIONS

The evaluation influence of the main parameters of the polymer layer of a rubber-metal vibration absorber, such as stiffness, dissipation, frequency and coefficient of friction, on its power characteristics and damping properties, allows us concluding that the developed model adequately simulates the operation of vibration dampers, gaskets and other power elements that have the properties of a polymer used for installation in various industries.

The paper found that:

- the following values of the main parameters of the Fancher spring can be taken:  $\mu = 0.8$ ;  $C_{fan} = 9 \cdot M \times N/m$ ;  $\beta = 0.000002$ ;  $k = -6 \cdot 10^{12} N/m$ ,
- an increase in the Maxwell cell dissipation coefficient leads to a decrease in the dependence of the stiffness and dissipation parameters on the frequency therefore, the shorter the relaxation time is, the more sensitive the element is to the frequency of vibrations,
- by varying the ratio of  $C$  and  $d$ , it is possible to determine the frequency limit at which the maximum damping should be achieved.

Due to the fact that it is planned to install polymer elements between the axle Assembly and the side frame of freight car bogies to reduce wear in the contact of the wheel and rail, the impact parameters of the polymer layer installed on the rolling stock gasket will be evaluated separately in the next article.

Analysis of the results of ride dynamics and of the impact on the bogie and switches tests of a gondola car equipped with bogies with diagonal links allowed us making the following conclusions:

- values ratio of frame forces to the static load from the wheelset on the rails and the coefficient of stability margin against the derailment of wheels in switches with rails of the P65 type with 1/9 and 1/11 grades up to a speed of 40 km/h, in a curve with a radius of 400 m and on a straight section of bogie meet the regulatory requirements,
- lateral forces on the switch with the 1/9 cross piece when a loaded gondola moves in a diverging direction at a speed of 50 km/h which exceeds the standard value by 20%. In this regard, it is recommended to limit the permissible speed of a loaded gondola car model on switches with a 1/9 cross piece in the diverging direction to a speed of 35 km/h,
- criterion of stability rail-bar grid against laterally shifting ballast on all experimental plots does not exceed standard values,
- dynamic linear load on the bogie meets the requirements of the established standards,
- smoothness indicators of the gondola car comply with regulatory requirements when it moves at speeds up to the design speed.

Based on all the above, it can be concluded that in general, gondola cars equipped with bogies with diagonal links between the side frames have improved dynamic qualities and can be allowed to operate on the main roads of the Commonwealth of Independent States.

#### ACKNOWLEDGMENTS

*This research was funded by the Almaty University of Power Engineering and Telecommunications.*

#### REFERENCES

- [1] ADILKHANOV Y., SEKEROVA S.H., MUSAYEV J., ZHAUYT A., YUSSUPOVA S., ALIMBETOV A., 2017, *Simulation Technique of Constant Contact Side Bearings of Freight Car Bogies*, Journal of Measurements in Engineering, 5/3, 142–151.
- [2] KAEWUNRUEN S., YOU R., ISHIDA M., 2017, *Composites for Timber-Replacement Bearers in Railway Switches and Crossings*, Infrastructures, 2/13, 1–17.
- [3] SCHEFFEL H., 1974, *Lateral Wobbles Stability and Rolling Stock Ability to Follow Curves*, Railway World, 12, 32–46.
- [4] MUSAYEV J., SOLONENKO V., MAHMETOVA N., KVASHNIN M., ALPEISOV A., ZHAUYT A., 2017, *Some Aspects of the Experimental Assessment of Dynamic Behavior of the Railway Track*, Journal of Theoretical and Applied Mechanics, 55/2, 421–432.
- [5] REMENNIKOV A.M., KAEWUNRUEN S., 2007, *A Review of Loading Conditions for Railway Track Structures Due to Train and Track Vertical Interaction*, Struct. Control Health Monit., 15, 207–234.
- [6] MUSAYEV J.S., SOLONENKO V.G., MAKHMETOVA N.M., BEKZHANOVA S.E., KVASHNIN M.YA., 2019, *The Method for Limiting Speed When Passing Turnouts of Railway Vehicles with Bogies of ZK1 Model*, News of the National Academy of Sciences of the Republic of Kazakhstan, Series of geology and technical sciences, 1/433, 151–162.
- [7] MUSAYEV J., ZHAUYT A., SAGATBEK M., MATIKHAN N., KALIYEV Y., NAURUSHEV B., 2016, *Seismic Resistance of Horizontal Underground Openings in Anisotropic Rocks*, Vibroengineering Procedia, 8, 231–236.
- [8] WANG Z., ZHANG Y., GUO J., SUN N., 2018, *Analysis on Transmission Characteristic of Integrated Track Circuit in Station*, Railway Development, Operations, and Maintenance, 2018, 19–27.
- [9] MUSAYEV J., ABILKAIYR Z.H., KAIYM T., ALPEISOV A., ALIMBETOV A., ZHAUYT A., 2016, *The Interaction of Freight Car and Way Taking Into Account Deformation of Assembled Rails and Sleepers*, Vibroengineering Procedia, 8, 269–274.

- [10] SHEN Y., ZHAO J., 2017, *Capacity Constrained Accessibility of High-Speed Rail*, Transportation, 44/2, 395–422.
- [11] ADILKHANOV Y., MURZAKAYEVA M., IGEMBAYEV N., ZHAUYT A., BUZAUOVA T., ORYMBAYEV S., 2019, *Experimental Researching of Dynamic Quality and Safety Movement of Half-Wagons Which Have Trolleys with Diagonal Connections*, Journal of Engineering and Applied Science, 14/16, 5831–5839.
- [12] KAEWUNRUEN S., REMENNIKOV A.M., 2009, *Dynamic Flexural Influence on a Railway Concrete Sleeper in Track System Due to a Single Wheel Impact*, Eng. Fail. Anal., 16, 705–712.
- [13] JENKINS H.H., STEPHENSON J.E., CLAYTON G.A., MORLAND J.W., LYON D., 1974, *The Effect of Track and Vehicle Parameters on Wheel/Rail Vertical Dynamic Forces*, Railw. Eng. J., 3, 2–16.
- [14] BODARE A., 2009, *Evaluation of Track Stiffness with a Vibrator for Prediction of Train-Induced Displacement on Railway Embankments*, Soil Dynamics and Earthquake Engineering, 29/8, 1187–1197.
- [15] CHOI J.Y., 2013, *Influence of Track Support Stiffness of Ballasted Track on Dynamic Wheel-Rail Forces*, Journal of Transportation Engineering, 139, 709–718.
- [16] BERGGREN E.G., KAYNIA A.M., DEHLBOM B., 2010, *Identification of Substructure Properties of Railway Tracks by Dynamic Stiffness Measurements and Simulations*, Journal of Sound and Vibration, 329, 3999–4016.
- [17] CLARK R., 2004, *Rail Flaw Detection: Overview and Needs for Future Developments*, NDT&E International, 37/2, 111–118.
- [18] ALVES COSTA P., CALC ADA R., CARDOSO A.S., BODARE A., 2010, *Influence of Soil Non-Linearity on the Dynamic Response of High-Speed Railway Track*, Soil Dynamics and Earthquake Engineering, 30/4, 221–235.
- [19] ABDELKRIM M., BONNET G., BUHAN P., 2003, *A Computational Procedure for Predicting the Long Term Residual Settlement of a Platform Induced by Repeated Traffic Loading*, Computers and Geotechnics, 30, 463–476.
- [20] ORLOVA A.M., BORONENKO YU.P., 2004, *Synthesis of Saved-Up Experience of Designing Trucks of Freight Cars for Developing a Typical Dimension Series*, Problems of Mechanics of Railway Transport, 2004, 45–55.
- [21] GALICHEV A.G., 2002, *Influence of Tribotechnical Condition of Wheels and Rails on Dynamics of Movement of Freight Locomotive*, Diss. of Cand.Tech. Sci., Bryansk State Techn. Univ., 2002, 34–42.
- [22] PRANOV A.A., YEFIMOV V.P., 2003, *Modernization of Truck of Model 18-100 as Effective Way of Increasing Traffic Safety of Trains*, Heavy Mechanical Engineering, 12, 75–85.
- [23] YEFIMOV V.P., PRANOV A.A., 2004, *Development and Carrying Out of Complex Testing of Truck of Model 18-578*, Problems of Mechanics of Railway Transport, 1, 123–135.
- [24] NIKIFOROV N.I., ZAGORSK M.V., SIMONOV V.A., 2002, *Studying the Influence of Parameters of the Mechanism of Radial Mounting of Wheel Pairs on Running Dynamics of Locomotive*, Transport, 6/52, 65–69.
- [25] SAMUELS J., POTASSIUM C., 2003, *Improvement of Interaction of Rolling Stock and Way*, Railroads of the World, 2, 18–24.
- [26] POLUKOSHKO S., 2016, *Estimation of Damping Capacity of Rubber Vibration Isolator's Under Harmonic Excitation*, Vibroengineering Procedia, 8, 50–56.
- [27] POLUKOSHKO S., MARTINOV S., SOKOLOVA S., 2017, *Aging, Fatigue and Durability of Rubber Vibration Isolation Elements*, Proceeding of the 11th International Scientific and Practical Conference: Environment, Technology, Resources, 3, 269–275.
- [28] POLUKOSHKO S. MARTINOV S. ZAICEVS E., 2018, *Influence of Rubber Ageing on Damping Capacity of Rubber Vibration Absorber*, Vibroengineering PROCEDIA, 19, 103–109.
- [29] MUSAYEV J., ADILKHANOV Y., ZHAUYT A., 2014, *Investigation of a Wedge Shock Absorber Trucks Freight Cars Using Universal Mechanism*, Middle-East Journal of Scientific Research, 22/9, 1405–1410.